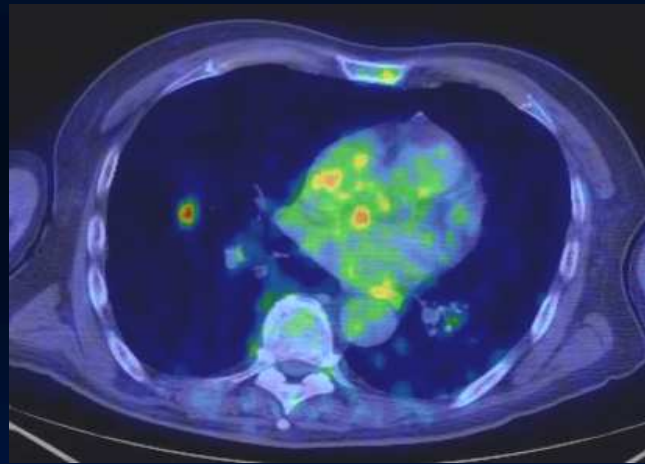


MOLECULAR METABOLIC IMAGING FOR RADIOTHERAPY PLANNING



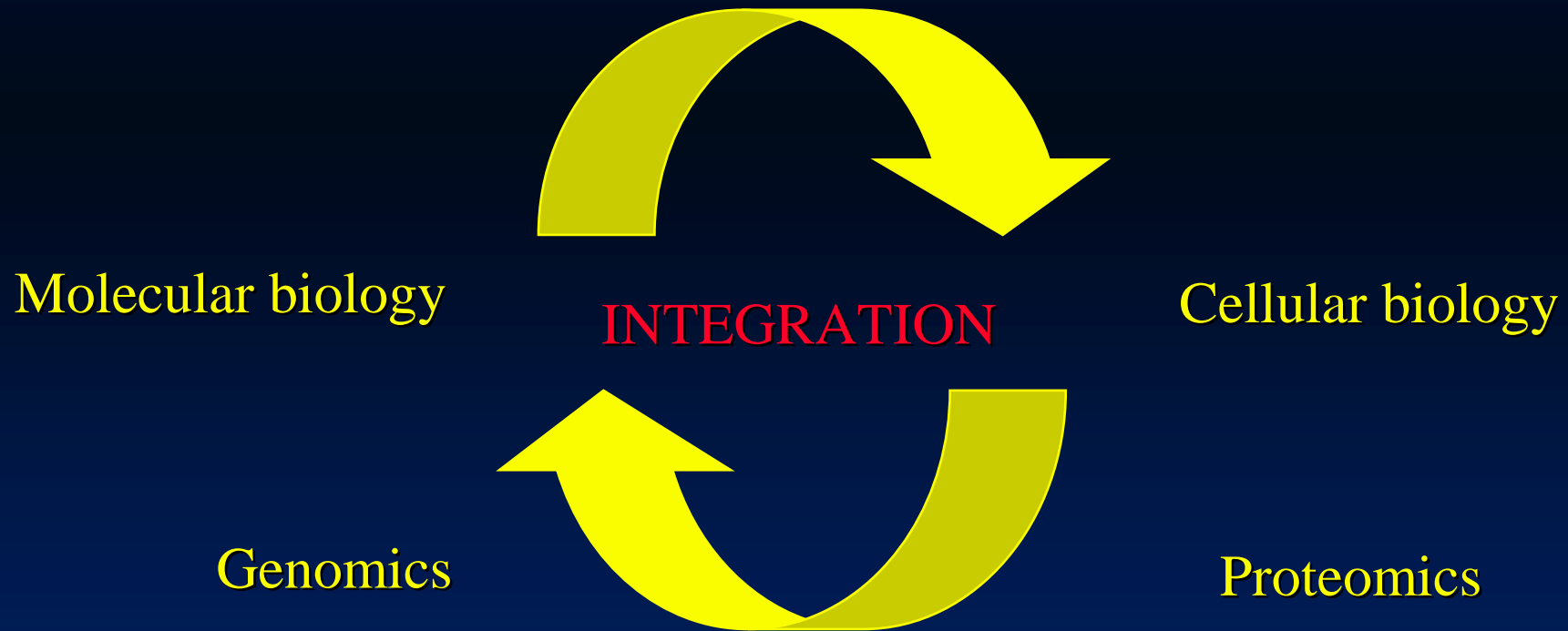
Isabella Castiglioni

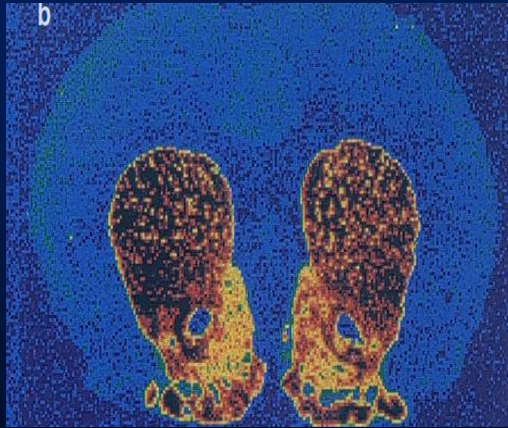
IBFM-CNR,

Scientific Institute H.S.Raffaele, University of Milan-Bicocca

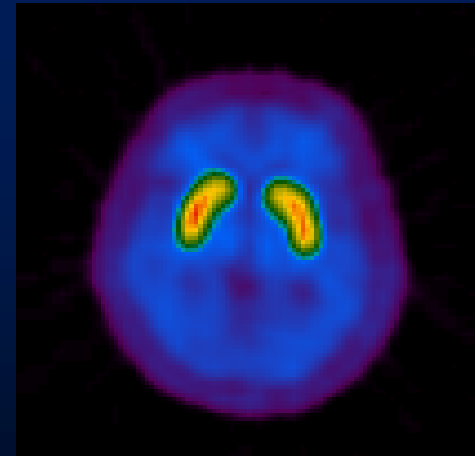
POST-GENOMIC MOLECULAR METABOLIC IMAGING

Molecular metabolic imaging

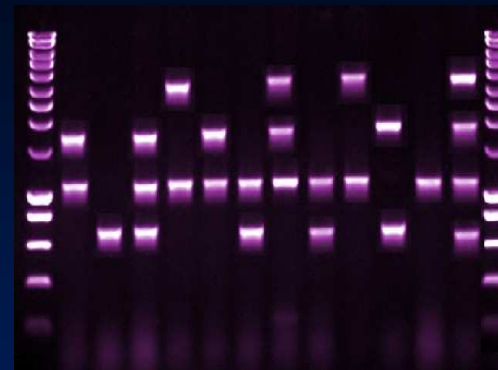
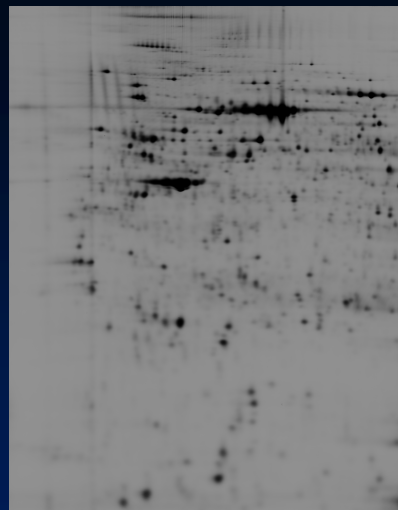




**EX-VIVO
HISTOPATHOLOGY**

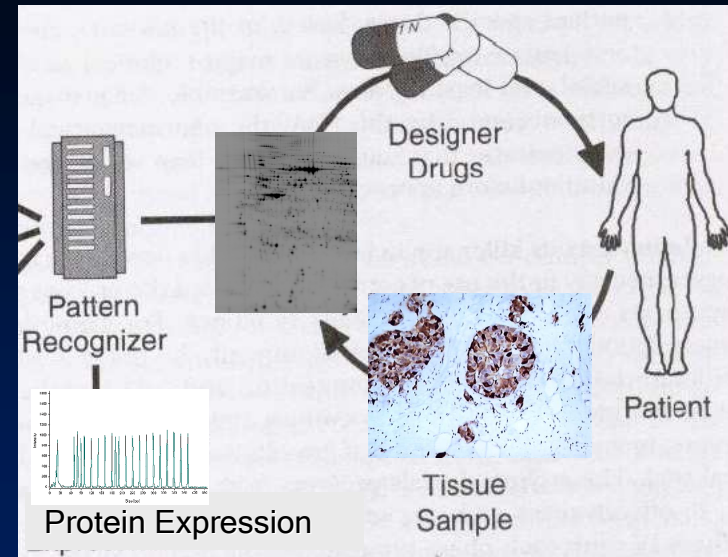
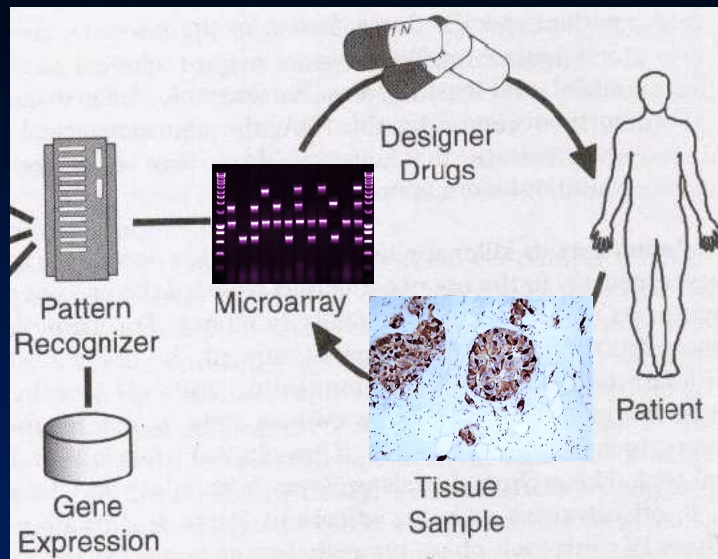
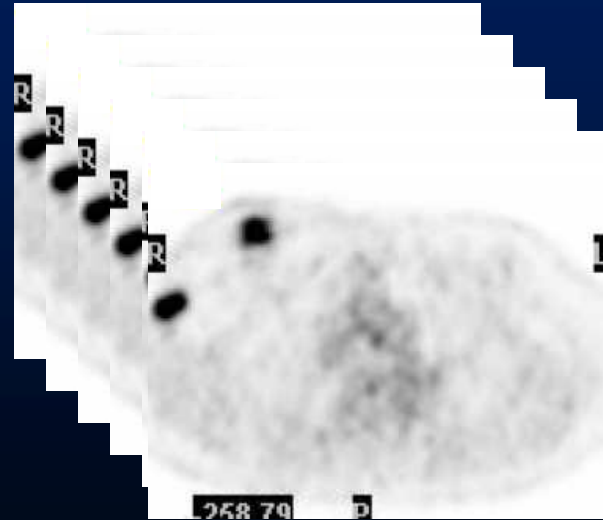
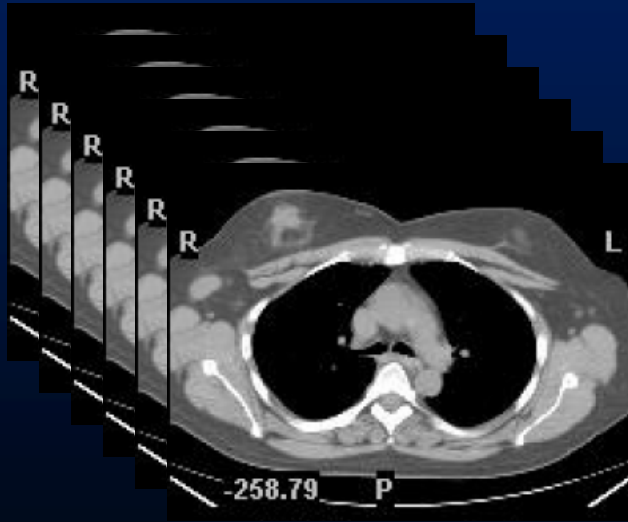


**IN-VIVO
HISTOPATHOLOGY**

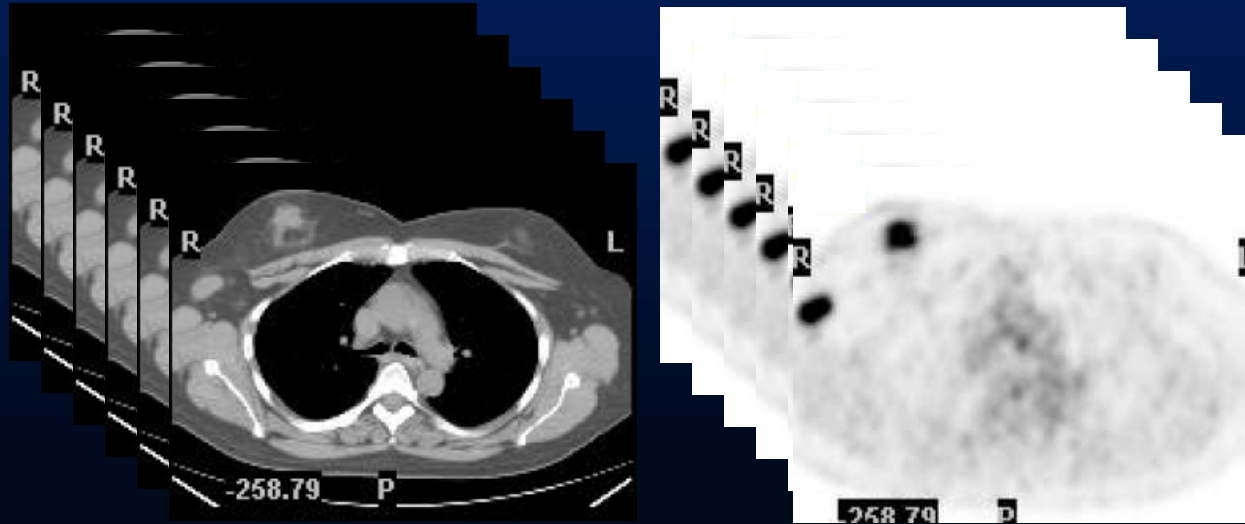


IN-VITRO HISTOPATHOLOGY

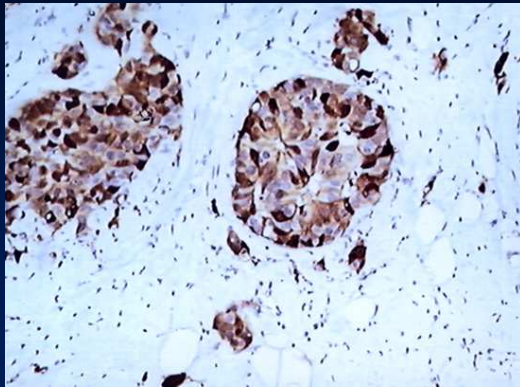
INTEGRATED PROTOCOLS



DATA TO BE INTEGRATED



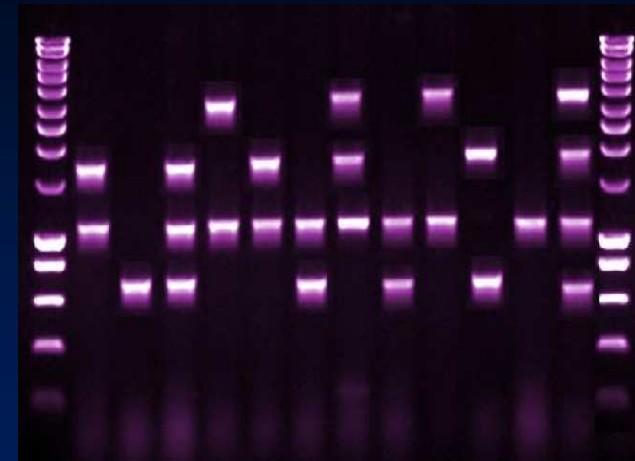
^{18}F -PET/CT glucose metabolism for breast carcinoma



pTnm



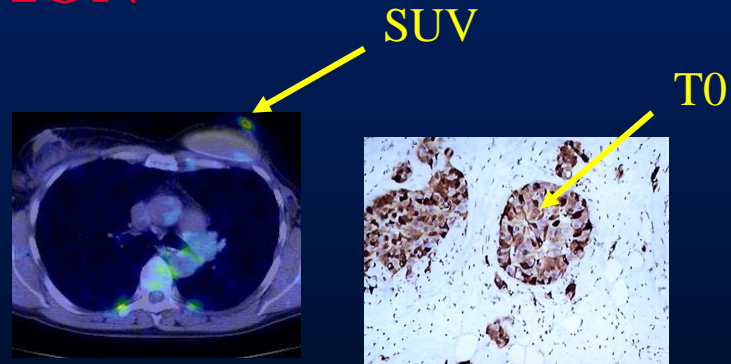
overexpressed proteins



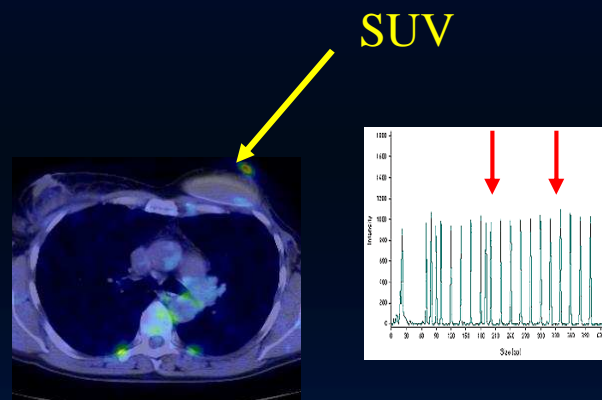
modified genes

INTEGRATION

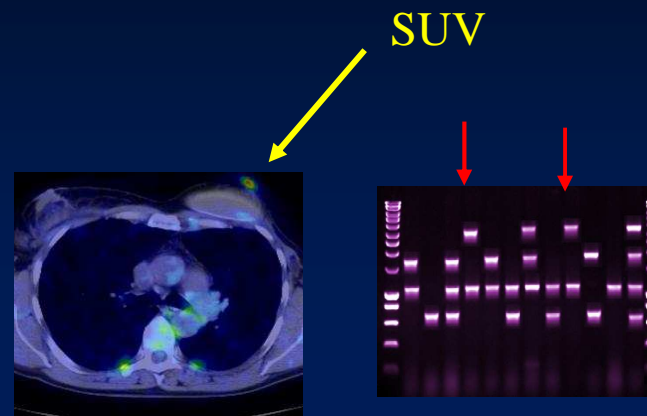
PET + vs Cancer aggressiveness



PET + vs Protein expression levels

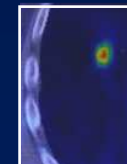
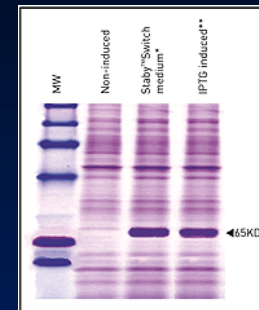
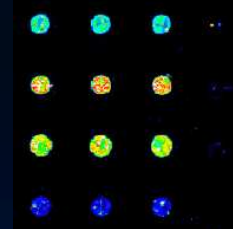
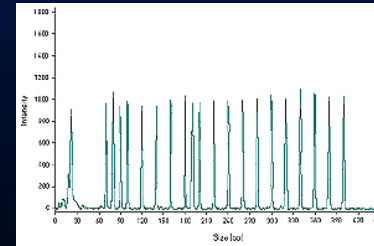
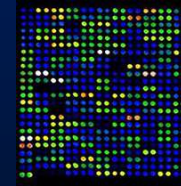
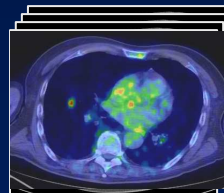
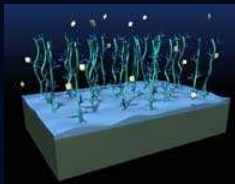
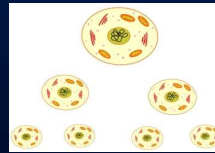
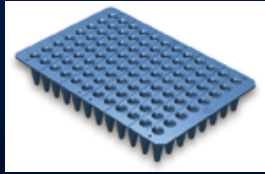


PET + vs modified genes

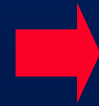


THE CHALLENGE

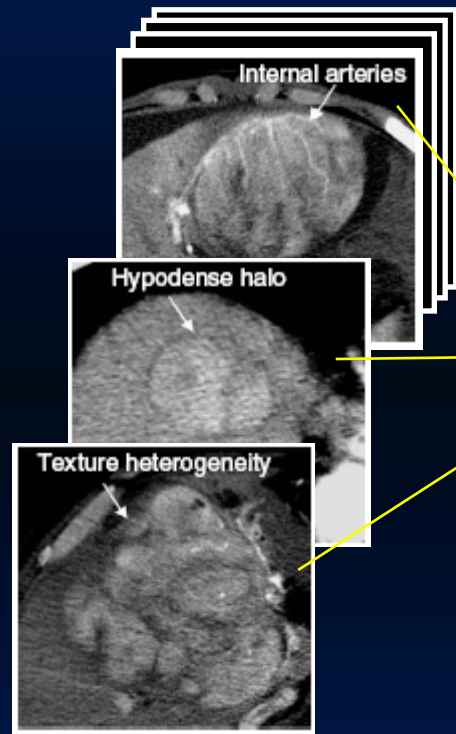
To determine genetic/biochemical characteristics *in vivo* & non invasively



A correlation exists between CT traits and gene expression in HCC cells

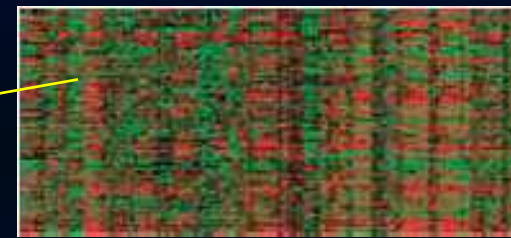


hepatic syntetic functions
cellular proliferation
prognostic factors

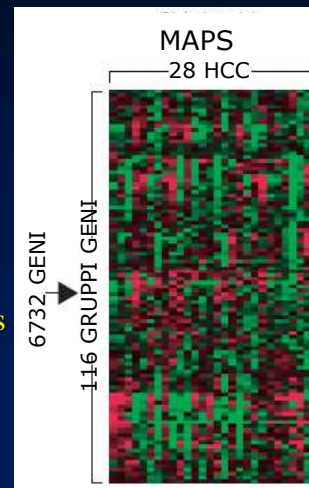


138 "traits" CT

Combinations, logical relations



6732 genes



Every gene group is associated with a combination of traits

GENE GROUPS	
■	Necrosis, percent
■	Internal septa
■	Texture heterogeneity, portal-venous phase
■	Tumor margin score, minimum
■	Enhancement pattern
■	Internal arteries, rank
■	Hypodense halo
■	Wash-out, maximum
■	Internal arteries, density
■	Tumor - liver difference, maximum
■	Corrected imaging area
■	Necrosis, density
■	Tumor margin score, maximum
■	Texture heterogeneity, arterial phase
■	Internal arteries, necrosis edge
■	Capsule
■	Wash-in, maximum
■	Infiltration, percent
■	Tumor - liver difference, minimum
■	Attenuation - heterogeneity score, maximum

RESULTS

28 informative HCC traits

116 groups of genes with coherent variations

POST-GENOMIC RADIOOTHERAPY

Radioterapia

Imaging Metabolico Molecolare

Biologia molecolare

Biologia cellulare

INTEGRAZIONE

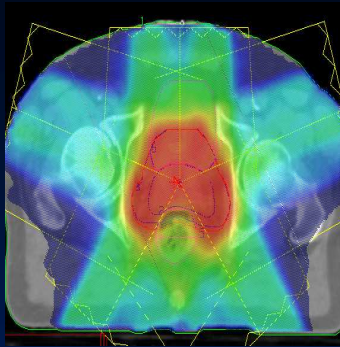
Genomica

Proteomica

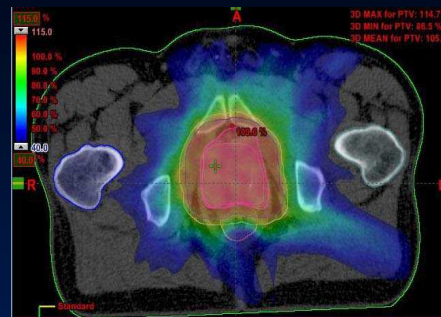


RADIOTHERAPY & HIGH TECH

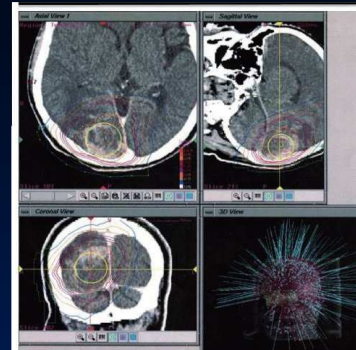
- High conformal radiation dose
- Steep dose gradients



IMRT



VMAT



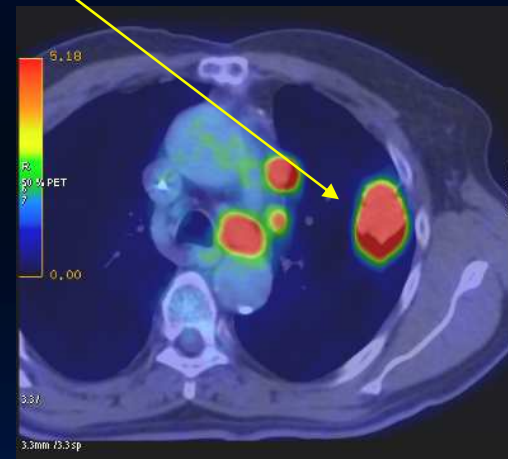
CK



HIT

MOLECULAR METABOLIC IMAGING for RADIOTHERAPY PLANNING

BTV



^{18}F -FDG PET

Molecular metabolic imaging: ^{18}F -FDG PET

- Efficacy of ^{18}F -FDG PET in a wide variety of malignant tumours
- Sensitivity, specificity and accuracy ~ 90%



- Better patient management and changes in the treatment plans in 25–50% of the cases

MOLECULAR METABOLIC IMAGING & HIGH TECH

Compensated lesion motion



4D PET/CT gating

Increased spatial resolution
(up to 3-4mm)

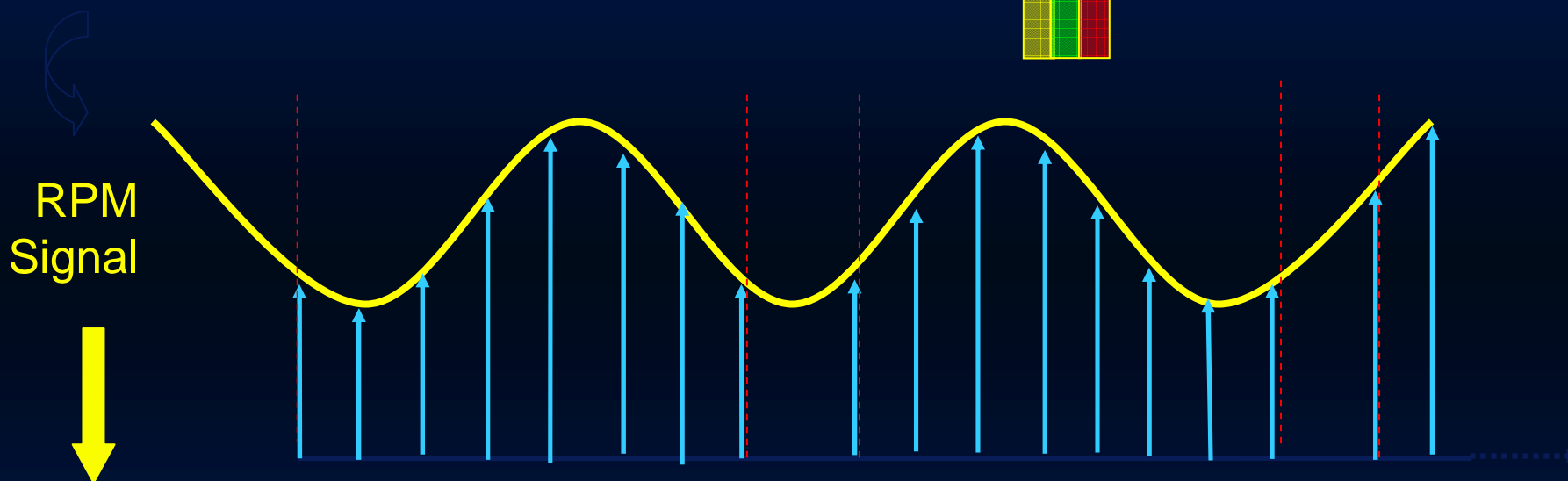
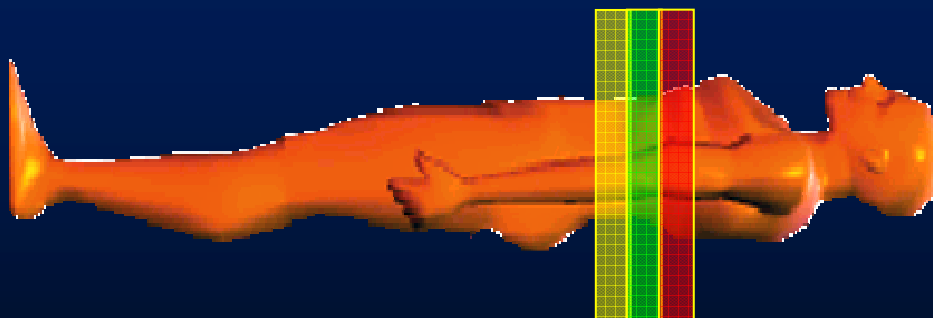
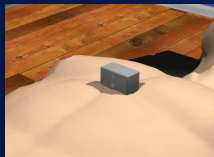


High-tech PET-CT systems
& improved reconstruction
algorithms



Better BTV definition

4D CT-PET Data Acquisition

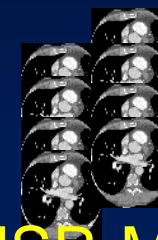
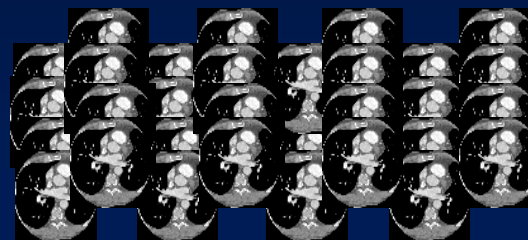
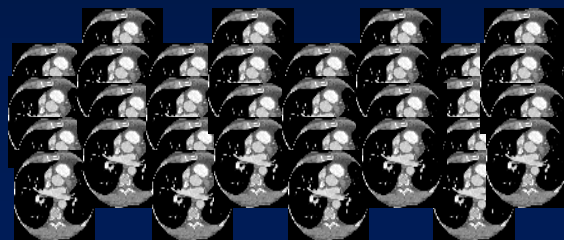


CT Acq.

Scan
First Position

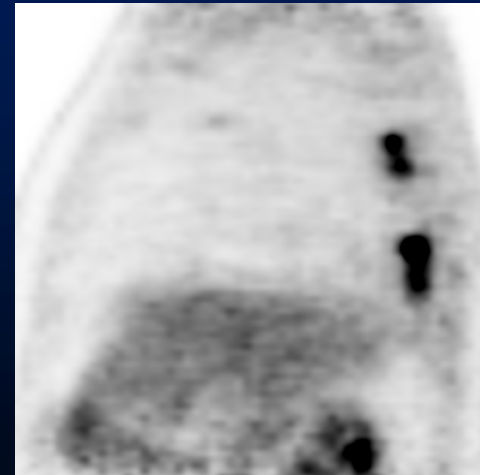
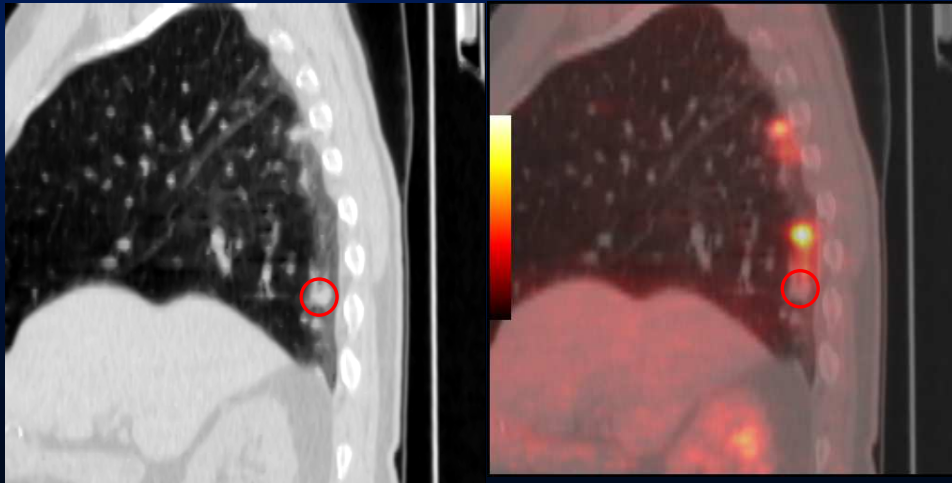
Scan
Second Position

Scan
.....

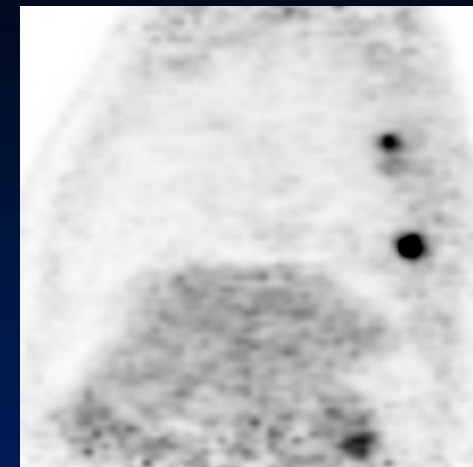
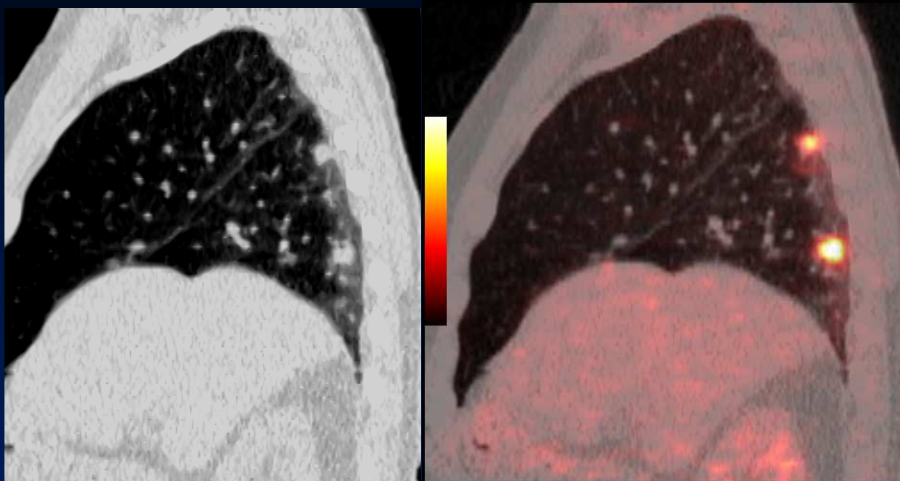


HSR-Milano

Conventional PET/CT



4D-PET/CT



HSR-Milano

BTV from PET images

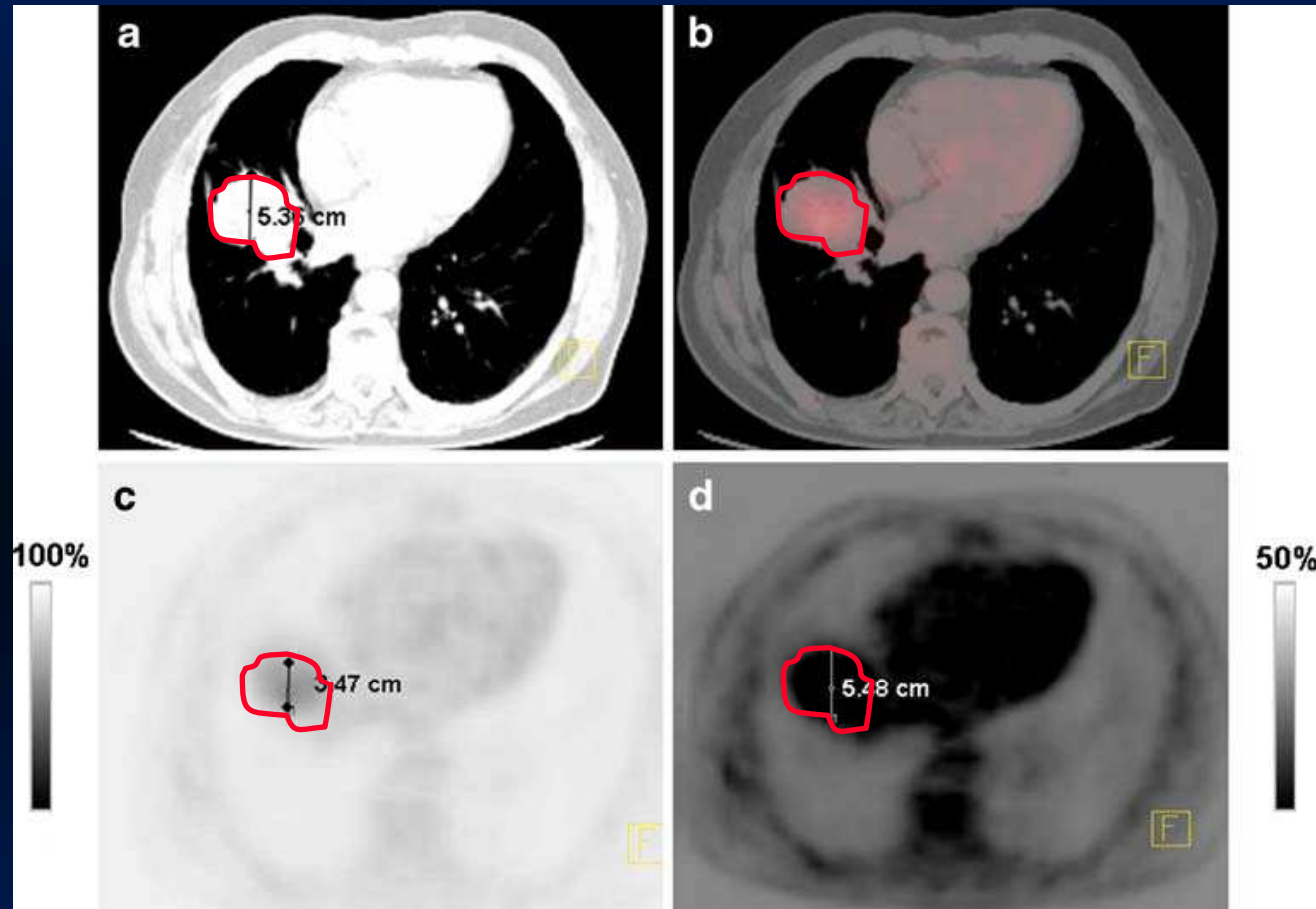
Segmentation techniques

Qualitative methods  Manual contouring

Quantitative methods  Semi-auto/image contouring

More reproducible, affordable

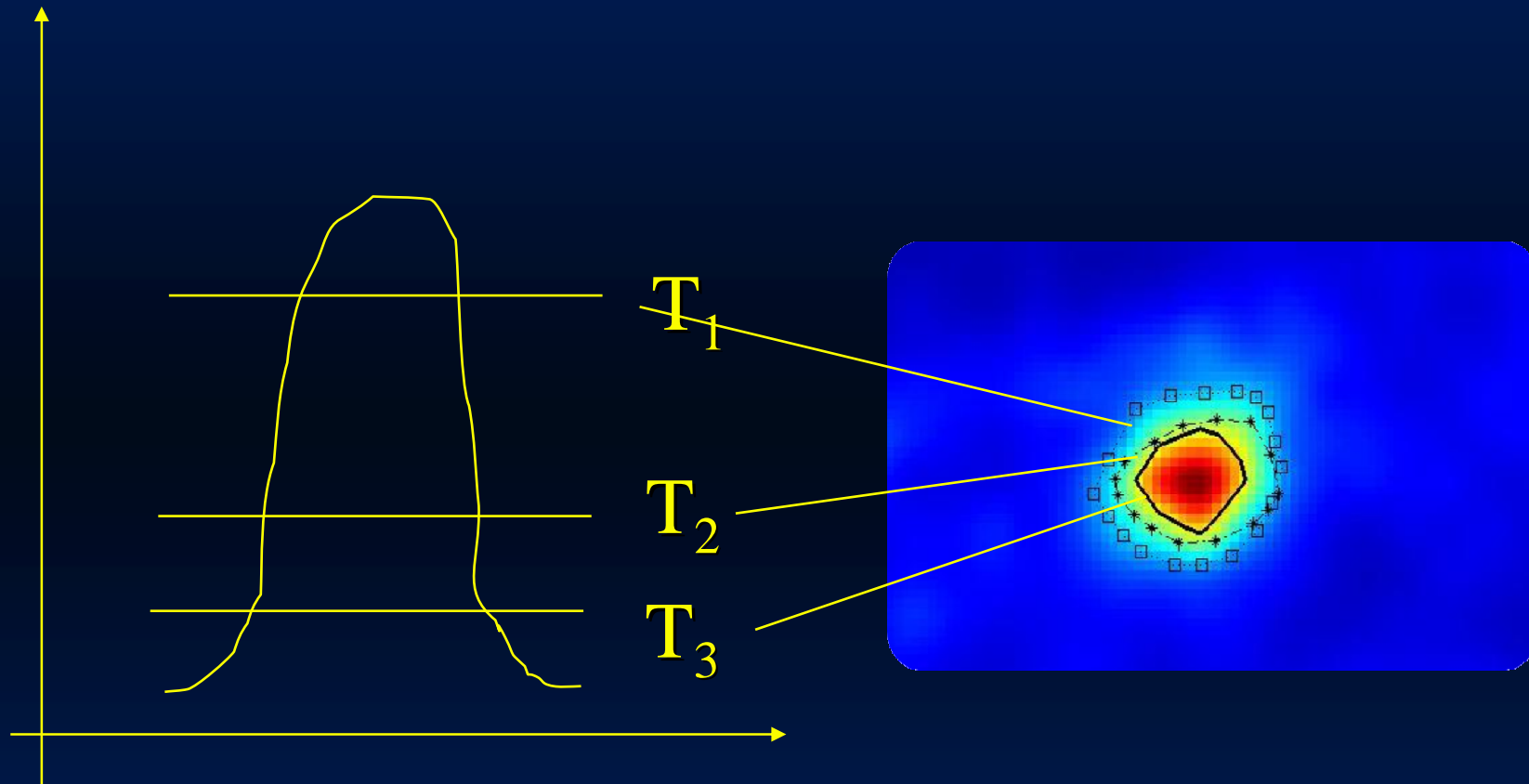
Qualitative methods



- Operator-dependent, image-modality dependent, image sampling dependent

Quantitative methods

Thresholding methods



$$\text{lesion} = T[I(\mathbf{x})] = \begin{cases} 1, & I(\mathbf{x}) \geq T \\ 0, & I(\mathbf{x}) < T \end{cases}$$

Thresholding methods

- absolute

$$T = 2,5 \text{ (SUV)}$$

- vs SUV

$$T = a + b \times \text{SUV}_{\text{mean}}$$

Black et al., 1990

- vs V

$$T = a + b \times \log_{10}(V) + q$$

Biehl et al., 2006; Ford et al., 2006

2d) vs LB (adaptative)

$$T = a + b \times 1/LB$$

Erdi et al., 1997

$$T = \text{Contrast level} \times (L_{\max} - B_{\text{mean}}) + B_{\text{mean}}$$

Drever et al., 2006

$$T = a \times L_{\text{mean-70\%}} + B_{\text{mean}}$$

Nestle et al., 2005

$$T = (a \times \text{SUV}_{\text{mean-70\%}} + b \times B_{\text{mean}}) / \text{SUV}_{\max}$$

Schaefer et al., 2008

$$T = b / LB + c$$

Daisne et al., 2003

2d) iterative

$$T = a/V + b / LB + c$$

Jentzen et al., 2007

$$T = a_0 + \exp[a + b/V + c \log V]$$

Nehmeh et al., 2009

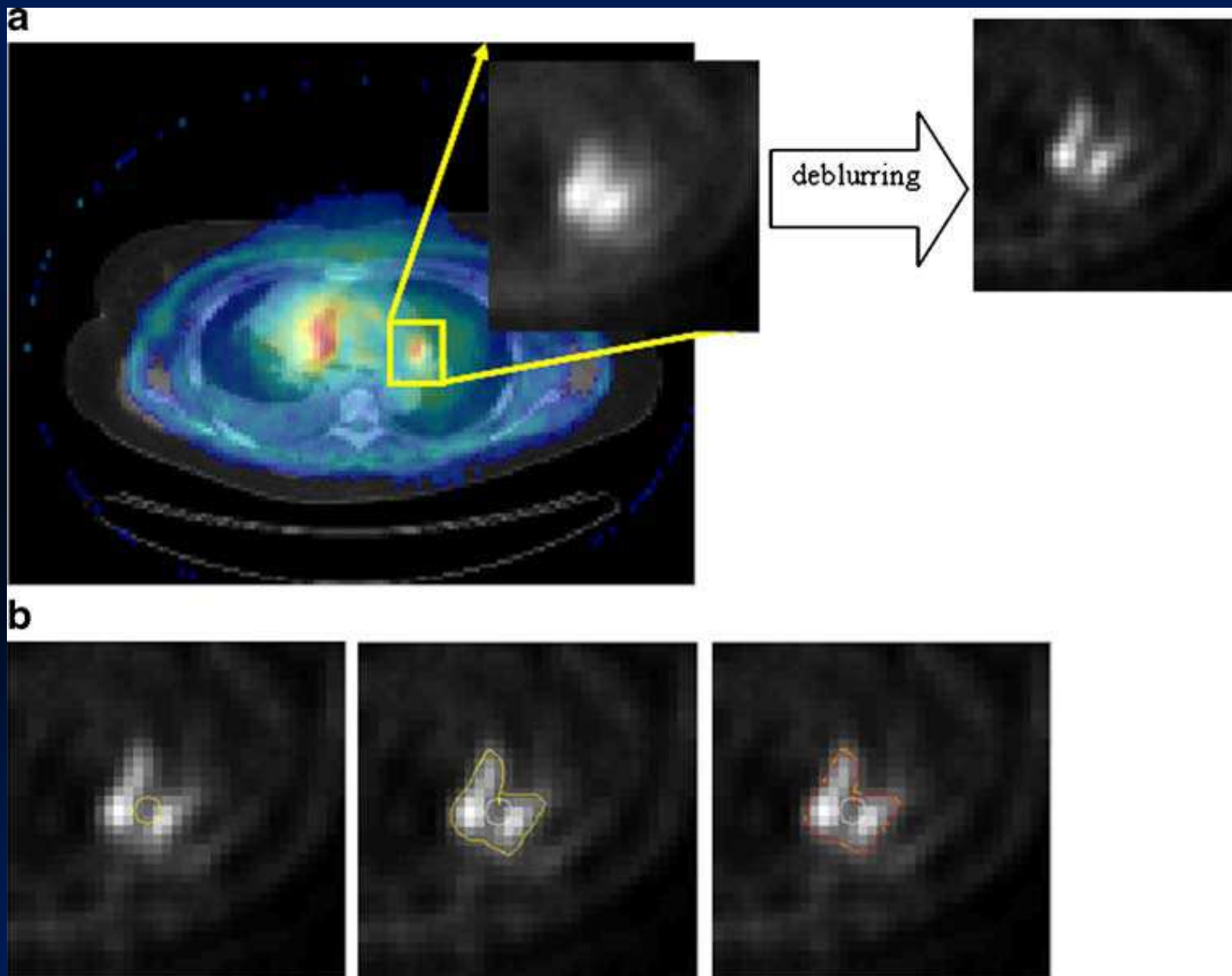
Variational

Geometric function of surface deforming under internal (surface bending characteristics) and external (directional gradients) forces

- edge detectors (Sobel operator) Drever et al. , 2007
- ridge detectors (Watershed Transform, WT) Drever et al. , 2007
- deformable active contour models (snakes) El Naqa et al. , 2007;
Li et al., 2008

Gradient Vector Flow (GVF), iterative evolutionary Poisson Differential Equation (up to the balance between internal and external forces) (e.g. level set method, deblurring algorithm)

level set method



1it

40 it

convergence

Learning methods

learning task aims to discriminate L from B based on a set of extracted features

Supervised

Training sets of labelled images
+ unknown samples

Classifiers

k-nearest neighbour (KNN)
Artificial neural network (ANN)
Support vector machine (SVM)

Unsupervised

Unknown samples

Belhassen et al. , 2010

Clustering

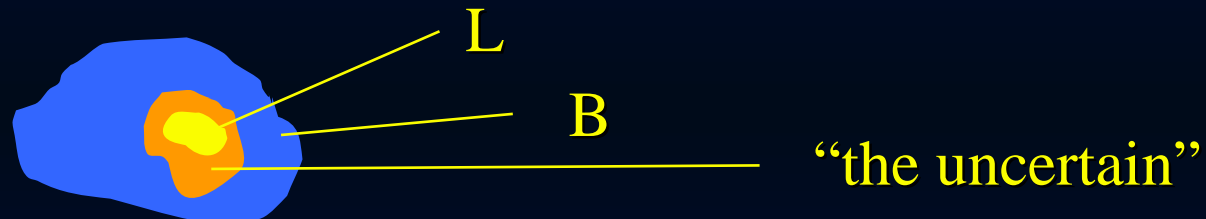
k-means
Fuzzy C-means (FCM)
Expectation maximization (EM)

Stochastic modeling

The intensity distribution of L and B are statistically different

Gaussian mixture model (GMM)

3 classes



EM (maximum likelihood) estimates the volumes by the probability of each voxel to belong to one of the three class

Validation of BTV in clinical studies is crucial and still limited

by histological specimens

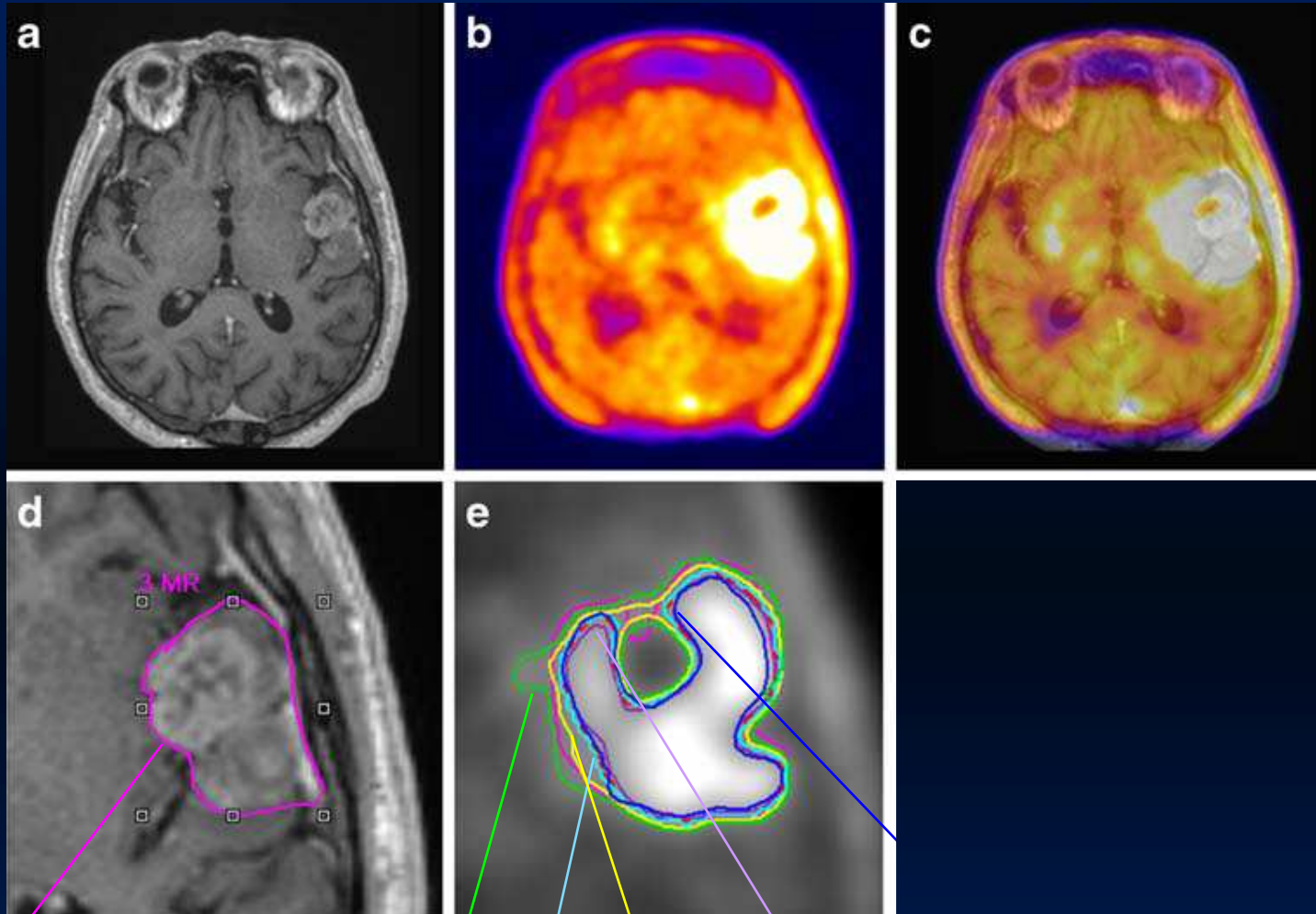
- PET reduces GTV
- PET BTV is more accurate with respect to CT/MRI GTV

Daisne et al., 2004

MRI

^{18}F -FET PET

MRI-PET



GTV_{MRI}

$\text{BTV}_{40\%}$

BTV_{LB}

BTV_{grd}

BTV_{man}

$\text{GTV}_{2,5}$

What is the best PET BTV?

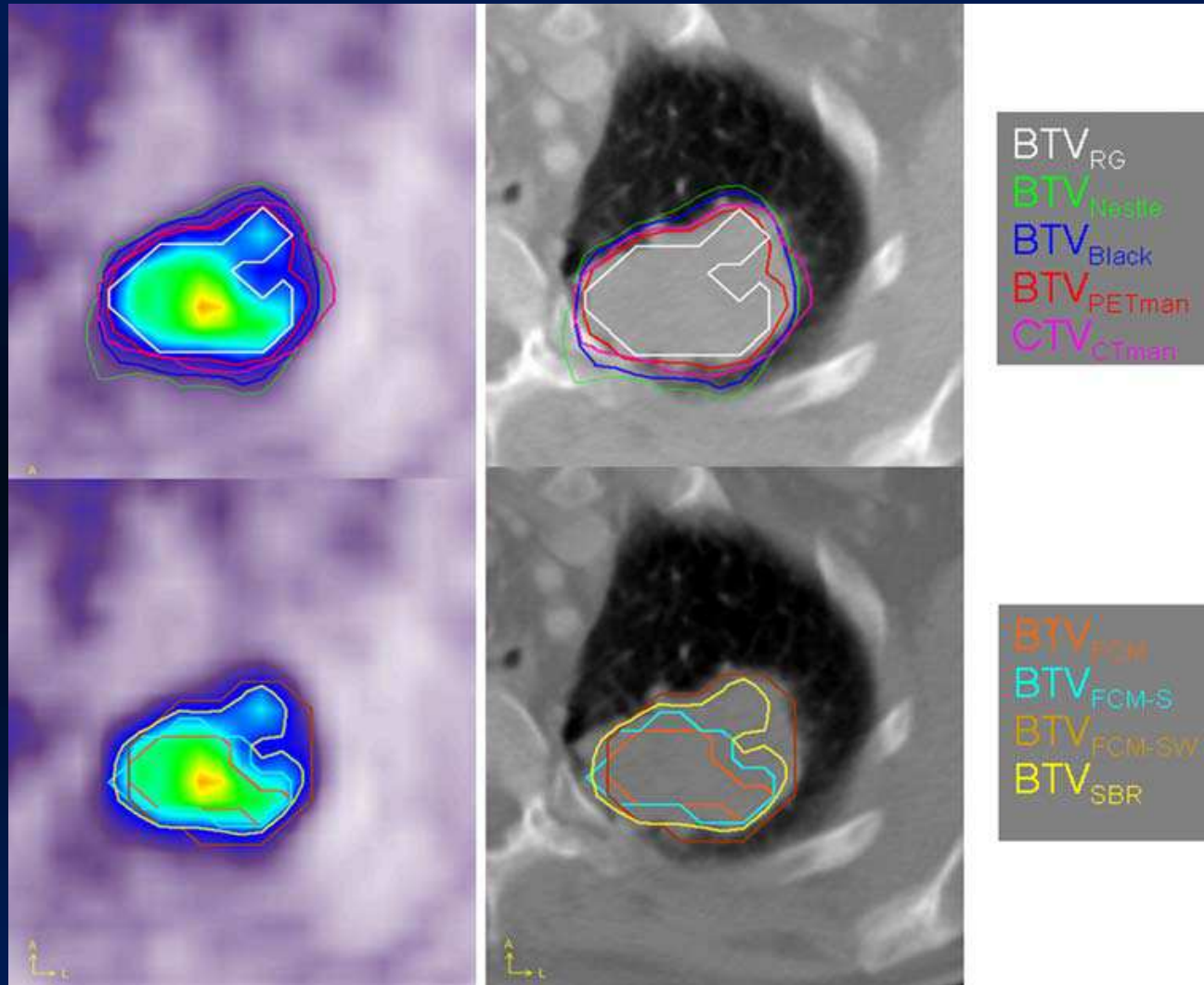
Validation of PET BTV in clinical studies is crucial and still limited

by histological specimens

- PET segmentation techniques extract similar d but different V

Belhassen et al., 2009

Comparison of 9 segmentation techniques



18F-FDG PET

CT

Belhassen et al., 2009

	d_{\max} (cm)	V (cc)
CT _{man}	6.5	98
PET _{man}	7.5	80
RG	6.0	61
Nestle	7.0	138
Black	6.5	117
SBR	6.5	65
FCM	4.8	32
FCM-S	5.5	45
FCM-SW	6.5	76

$$d_{GS}=7\text{cm}$$

PET Radiotracers

Tumour proliferation

^{68}F -Fluorotimidine

Aminoacid metabolism

*^{68}F -Fluoroethyltyrosine, ^{11}C -methionine,
 ^{11}C -tyrosine*

Cell membranes/ fatty
acid metabolism

^{11}C -acetate, ^{11}C -Choline, ^{18}F -Choline

Somatostiatin receptors

^{68}Ga -DOTA-TOC

Apoptosis

^{18}F -Annexin V

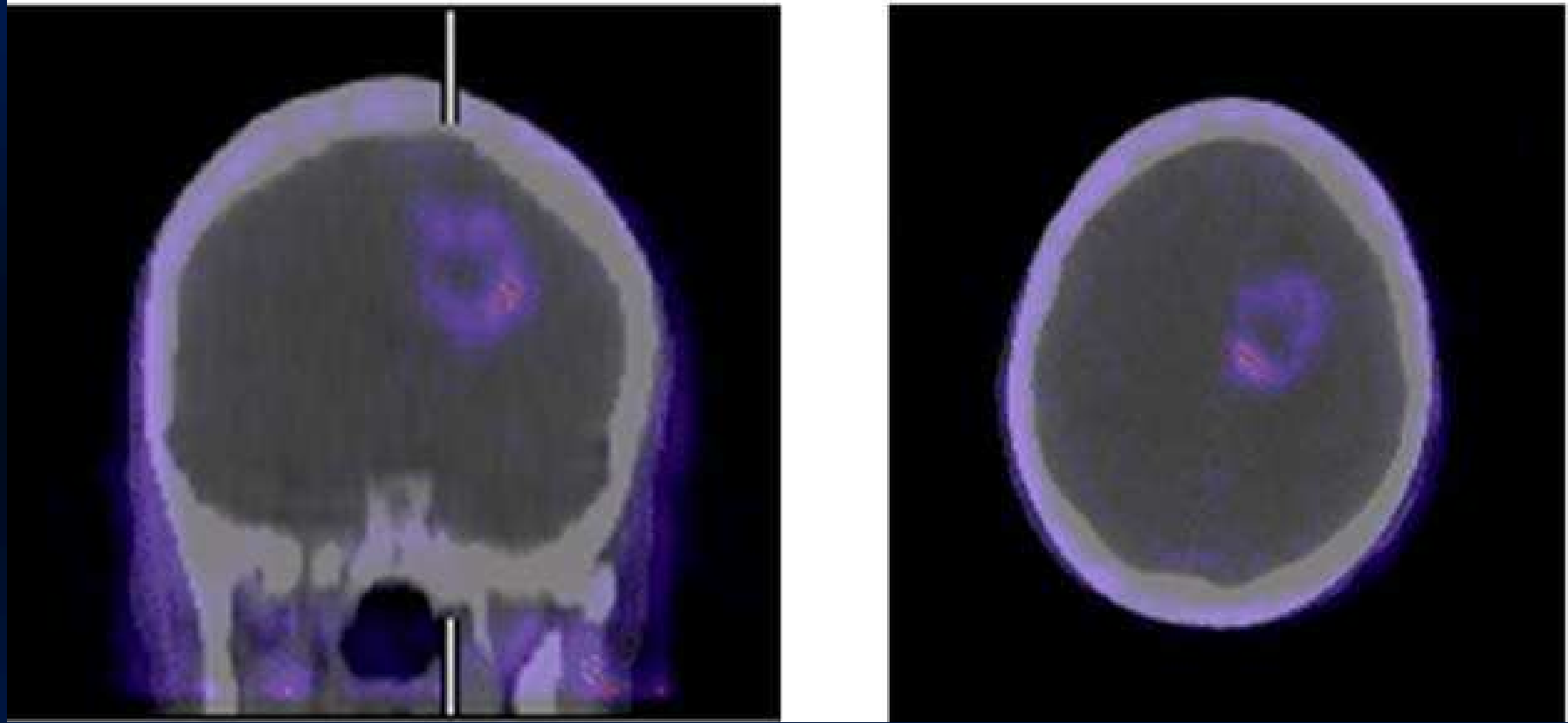
Angiogenesis

^{18}F -RGD peptide

Hypoxia

*^{18}F -FMISO, ^{11}F -FAZA, ^{64}Cu -ATSM,
 ^{18}F -EF3, ^{18}F -EF5*

^{18}F -FAZA PET-CT



glioma

Postema et al., 2009

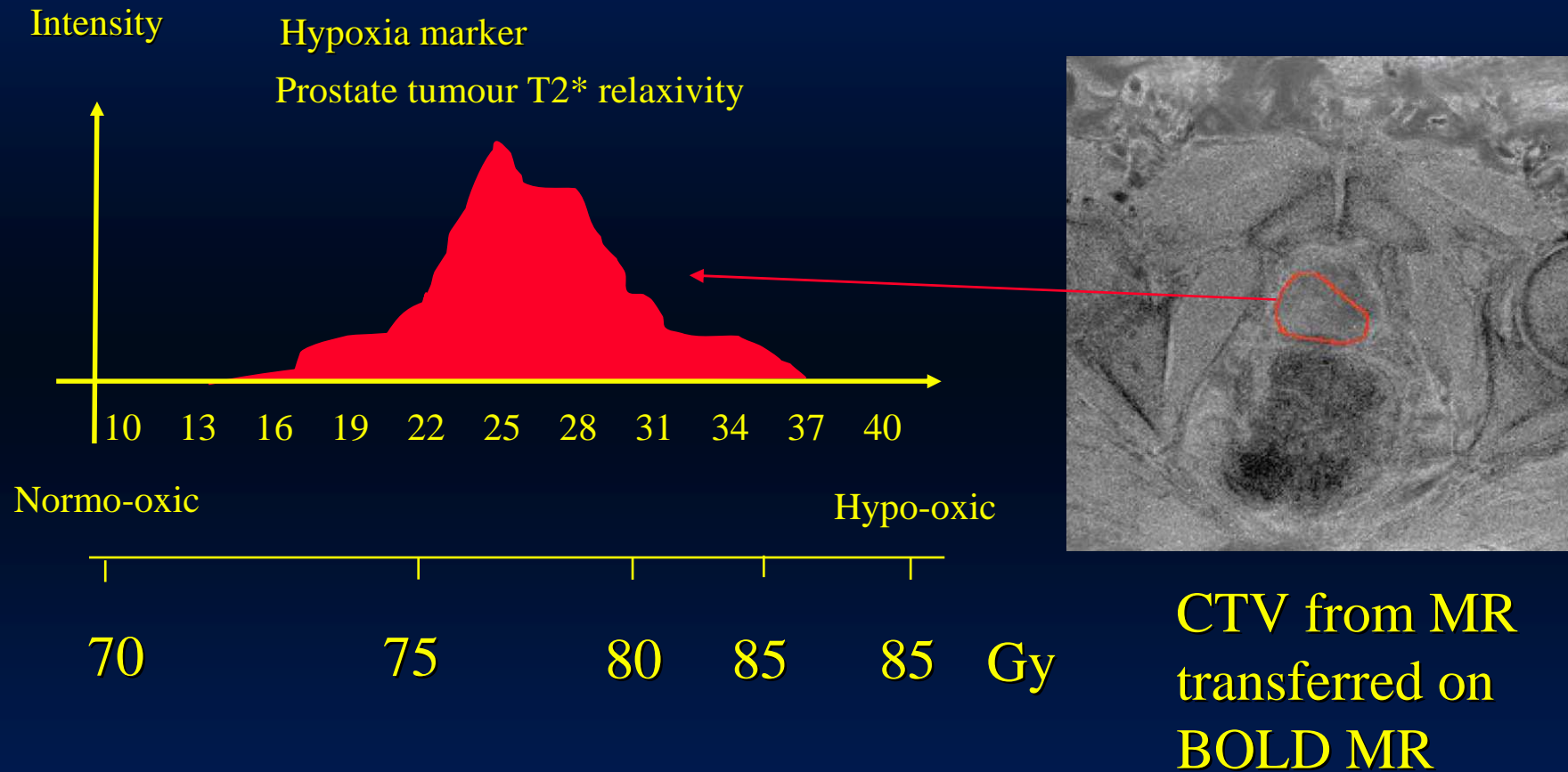
Hypoxia affects outcome of radiotherapy treatment

e.g. Nordsmark et al., 1996, 2000; Jomathan et al., 2006

Reduced perfusion correlate with therapy failure

e.g. Hermans et al., 2003; Vauper et al., 2004, 2005

“Dose painting by numbers” (Bentzen et al. *Lancet oncol*, 2005)



inverse treatment-planning : pixel-driven dose distribution

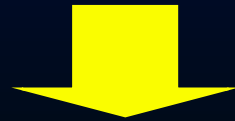
Are we ready with dose painting by numbers?

- 1) Assess temporal and spatial stability of PET hypoxia maps
- 2) Assess time of reoxygenation of hypoxic areas
- 3) Improve quantification of PET hypoxia maps

1) Assess temporal and spatial stability of hypoxia maps

Hypoxia: 100 μ m

Intermittent hypoxia: minutes-hours



Hypoxia and normoxic areas can coexist in one PET voxel



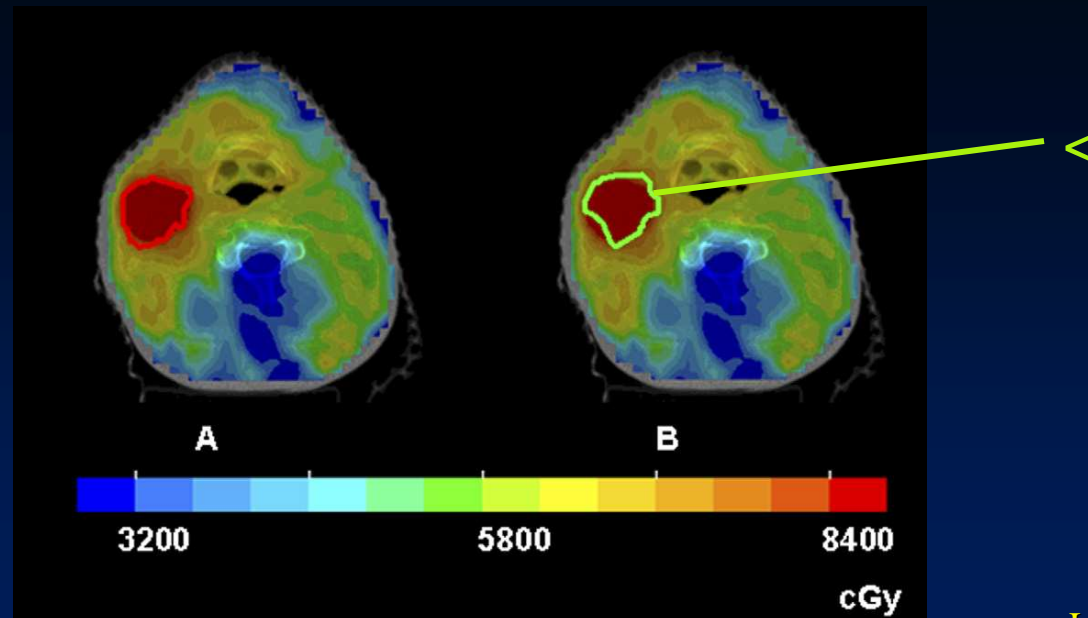
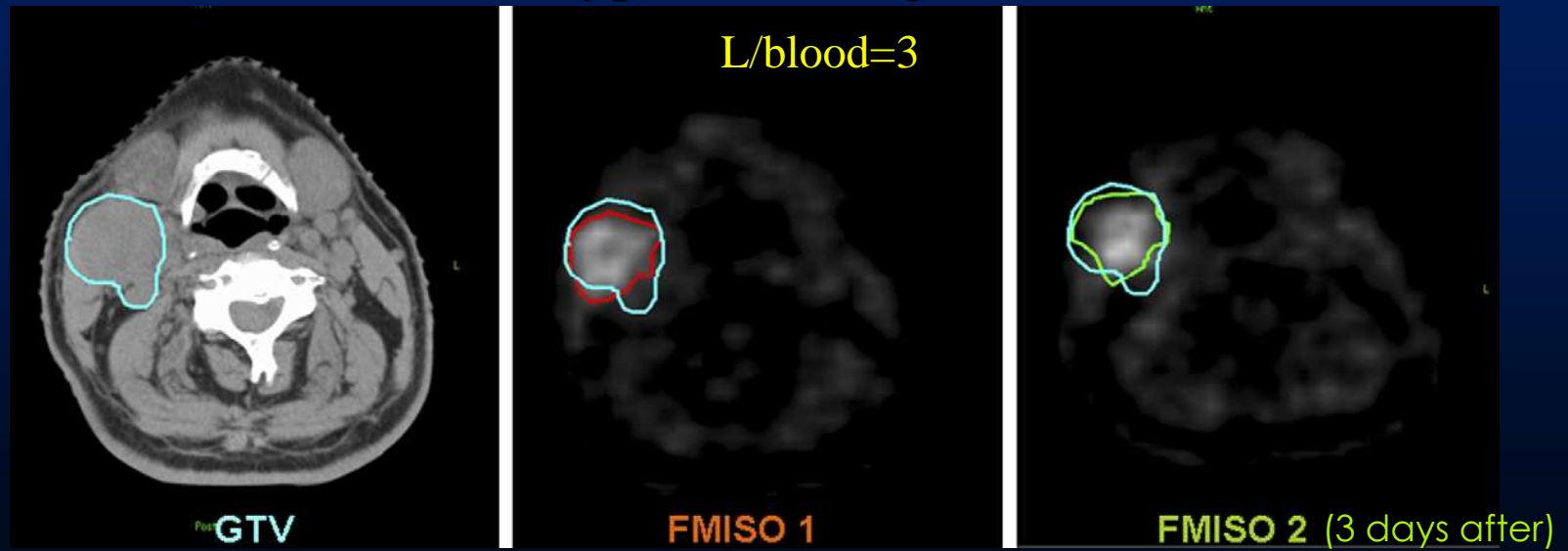
Multiparametric imaging (Dynamic/Multimodal (PET and CT/MRI))

2) Assess time of reoxygenation of hypoxic areas



Multiple imaging sessions during RT

Hypoxia during RT

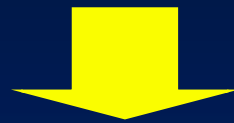


Time of reoxygenation depends inversely from perfusion efficiency

Cell sensitivity depends from tracer retention

Early PET scans

Late PET scans



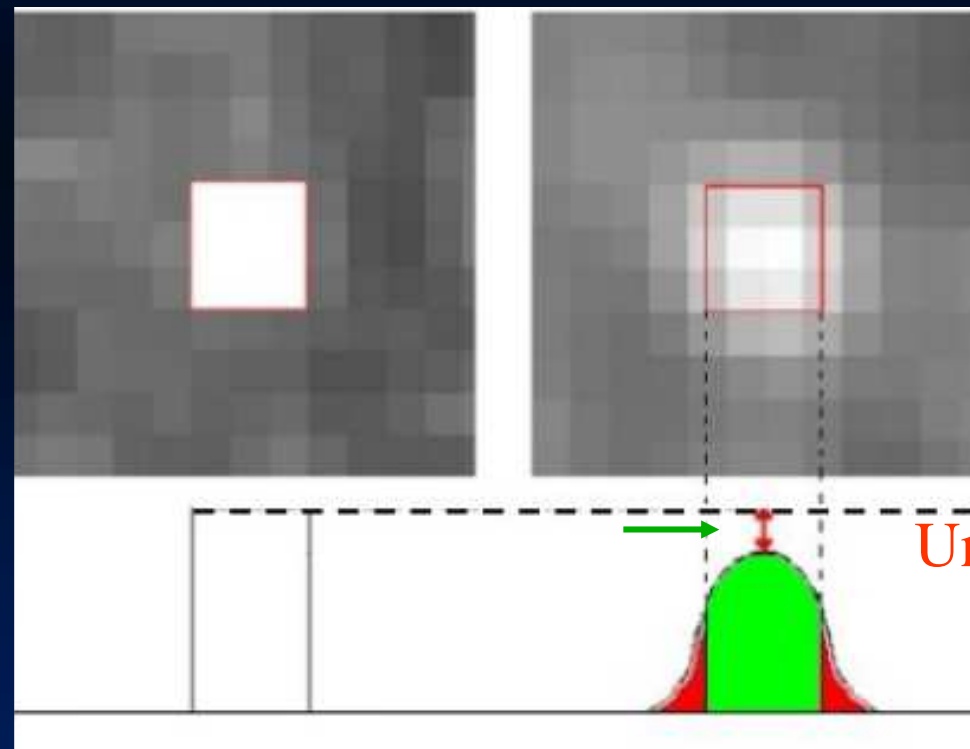
TCP can be used to stratify patients vs RT

3) Improve quantification of PET hypoxia maps

PET Partial Volume Effect

Ideal lesion

Real lesion

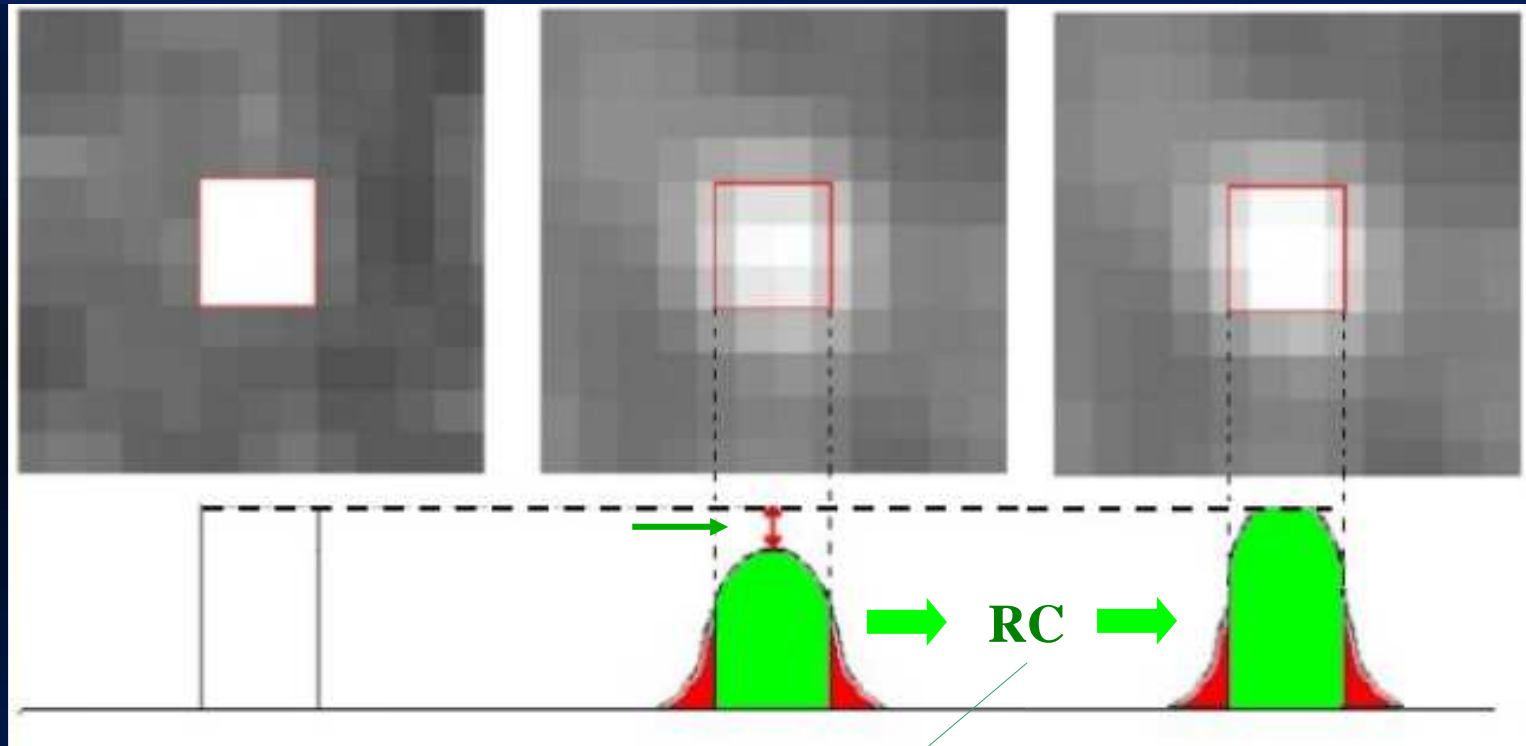


PVE PET correction

Ideal lesion

Real lesion

Corrected lesion



Measurement of RECOVERY COEFFICIENTS
(taking account of the system state)

Methods

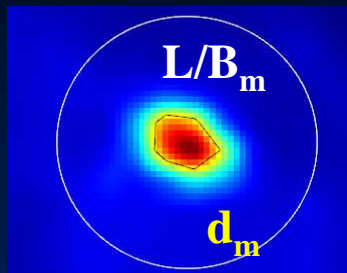
Recovery coefficients (RC) and RC curves from NEMA 2001 IQ phantom

$$RC = \frac{S/B_m}{S/B_{GS}}$$

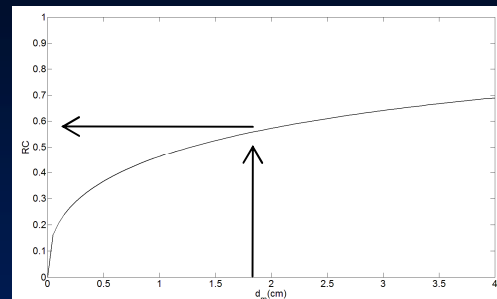
*GS = Gold Standard

RC function of measured sphere diameter (equivalent to V_m) and S/B_m

RC-based PVE correction method



RC



L/B_m



$$C_{\text{corrected}} = \frac{C_{\text{uncorrected}}}{RC}$$
$$SUV_{\text{corrected}} = \frac{SUV_{\text{uncorrected}}}{RC}$$

Castiglioni et al., 2009

Dose by BTV



Segmentation of qualitative PET metabolic images

Dose by BTV &
subvolumes



Segmentation of qualitative PET hypoxia images

(“dose painting”)

(Lyng et al. *Int J Radiat Oncol Biol Phys*, 2000)

Dose by PTV &
numbers



Quantitative PET hypoxia images

(“dose painting by
numbers”)

(Bentzen et al. *Lancet oncol*, 2005)

Dose by PTV & numbers (“dose painting by numbers”)

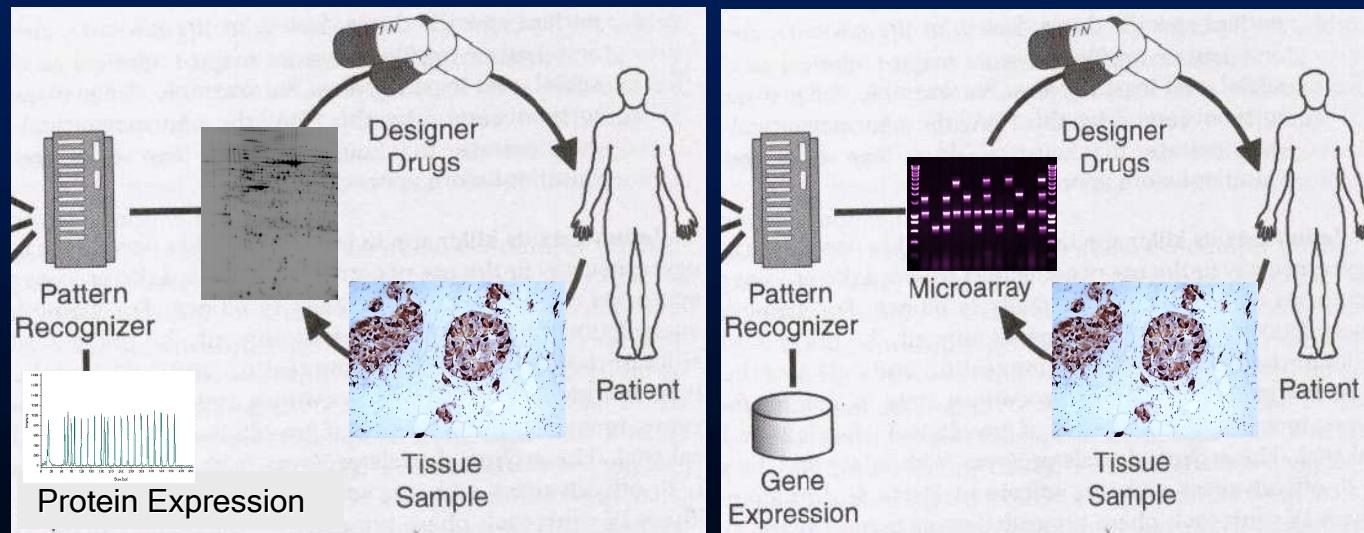
numbers = (PET voxels accurate numbers)

addressing to RT

RT planning

RT monitoring

Molecular imaging for RT



Ethiology, prognosis, tumour response to therapy

Personalized therapy periodically monitored

